DEUTSCHES ELEKTRONEN-SYNCHROTRON DESY

DESY 82-079
December 1982

GLUEBALL SPECTROSCOPY IN 4-d SU(3) LATTICE GAUGE THEORY I

by

B. Berg

II. Institut für Theoretische Physik der Universität Hamburg

A. Billoire

CEN Saclay, Gif-sur-Yvette

NOTKESTRASSE 85 · 2 HAMBURG 52

To be sure that your preprints are promptly included in the
HIGH ENERGY PHYSICS INDEX ,
send them to the following address (if possible by air mail) :

DESY
Bibliothek
Notkestrasse 85
2 Hamburg 52
Germany

DESY 82-079
December 1982

Glueball Spectroscopy in 4-d SU(3) Lattice Gauge Theory I

by

B. Berg [1] and A. Billoire [2]

1) II. Institut für Theoretische Physik der Universität Hamburg, Luruper Chaussee 149, D-2000 Hamburg 50

2) CEN Saclay, BP No. 2, F-91190 Gif-sur-Yvette, France

Abstract

We give a complete classification of states that can be constructed from spacelike Wilson loop operators up to length 8. This set of operators is considered in a Monte Carlo variational calculation.

In part I of this paper we report Monte Carlo results from an $4^3 \cdot 8$ lattice, relying on Wilson loops up to length 6. We find a scaling window for the 0^{++} state, but no scaling for any other state.

I. Introduction:

About ten years ago the existence of glueballs within QCD was suggested by Fritzsch and Gell-Mann [1]. Nowadays Monte Carlo (MC) calculations [2] within lattice gauge theories without quarks seem to be close to the point, that reliable results for the continuum limit may be obtained. A more careful discussion is given in section IV.a. The SU(2) and SU(3) glueball spectrum has been investigated by a variety of methods [3], in particular by means of MC variational (MCV) calculations [4-10].

In this paper we consider 4-d SU(3) lattice gauge theory with the Wilson action. At each link b of a hypercubic 4-d lattice there is an element $U(b) \in SU(3)$ and averages of gauge invariant operators are calculated with the partition function

$$Z = \int \prod_b dU(b) \exp\left\{-\frac{\beta}{3} \sum_p \mathrm{Re}\,\mathrm{Tr}\,(1 - U(p))\right\} \qquad (I.1)$$

For each plaquette p, U(p) is the ordered product of the four link matrices surrounding the plaquette and dU is the SU(3) Hurwitz [11] measure. We restrict ourselves to finite lattices of size $L^3 \cdot L_t$ with periodic boundary conditions.

With $\beta = 6/g^2$ the standard definition of the lattice mass scale is (a lattice spacing)

$$\Lambda^L = a^{-1} (\beta_0 g^2)^{-\frac{\beta_1}{2\beta_0^2}} \exp\left(-\frac{1}{2\beta_0 g^2}\right) \left(1 + O(g^2)\right), \qquad (I.2)$$

where

$$\beta_0 = \frac{11}{3}\left(\frac{3}{16\pi^2}\right) \quad \text{and} \quad \beta_1 = \frac{34}{3}\left(\frac{3}{16\pi^2}\right)^2.$$

The Λ parameters of perturbation theory can be related to Λ^L. For SU(3) $\Lambda^{MOM} = 83.4\,\Lambda^L$ [12]. At present experimental measurements indicate only the crude estimate [13]

$$\Lambda^L = (4.1 \pm^{2.6}_{1.1})\ \text{Mev}. \qquad (I.3)$$

We are interested in an MCV calculation of the SU(3) mass spectrum. States of this spectrum are called glueballs [1]. They are mesons described by the quantum numbers J^{PC} (J = spin, P = parity, C = charge parity). If the (quantum) continuum limit $\beta \to \infty$ of SU(3) lattice gauge theory exists, then all physical masses become in this limit proportinal to the lattice scale:

$$m(J^{PC}) = c(J^{PC}) \cdot \Lambda^L . \qquad (I.4)$$

The problem of spectroscopy is to calculate the constants $c(J^{PC})$. The mass gap m_g is the lowest lying glueball state which we conjecture to be the $m(0^{++})$ state.

Let us consider the variational definition of the mass gap

$$m_g = -a^{-1} \ln\left\{ \max_{\substack{|\psi\rangle \\ \langle 0|\psi\rangle = 0}} \frac{\langle\psi|T|\psi\rangle}{\langle\psi|\psi\rangle} \right\} \qquad (I.5)$$

Here $T = e^{-aH}$ is the transfer matrix [14] which connects spacelike planes at distance $\Delta t = a$. In the following we use often units $a = 1$. The vacuum $|0\rangle$ is the highest eigenstate of the transfer matrix and we choose the normalization $T|0\rangle = |0\rangle$. With a complete set of gauge invariant operators F_i (i = 1,2, ...), satisfying $\langle 0 | F_i | 0\rangle = 0$, the generic wave function if obtained as linear combination

$$|\psi\rangle = \sum_\lambda c_\lambda F_\lambda |0\rangle \qquad (c_\lambda \in \mathbb{C}). \qquad (I.6)$$

A complete set of states is obtained by taking as operators F_i products of different spacelike Wilson loops in all possible SU(3) representations:

$$O_{i,\nu}(\vec{x},t) = \chi_\nu\Big(\prod_{C_i} U\Big) - \langle 0|\,\chi_\nu\Big(\prod_{C_i} U\Big)\,|0\rangle \,. \qquad (I.7)$$

Here ν labels the SU(3) representations and i labels the closed spacelike paths $C_i = C_i(\vec{x},t)$. For $\vec{x}$ we take the center of the path. In this paper we are only interested in momentum $\vec{p} = 0$ states. In that case it is sufficient to consider operators

$$O_{i,\nu}(t) = \sum_{\vec{x}} O_{i,\nu}(\vec{x},t) \,. \qquad (I.8)$$

In an MCV calculation one truncates the set of operators. The relevant expectaion values

$$\langle 0|\,O_{i,\nu}(0)\,T\,O_{j,\mu}(0)|0\rangle = \langle 0|\,O_{i,\nu}(0)\,O_{j,\mu}(1)|0\rangle \qquad (I.9)$$

are calculated by means of MC measurements. If MC statistics allows various obvious consistency checks (which may considerably improve the final value) are obtained by including expectation values $\langle 0|O_{i,\nu}(0)\,O_{j,\mu}(t)\,|\,0\rangle$ at distance t = 2,3 in the analysis. By practical reasons one is limited to a rather small number of allowed operators, and in particular only the Wilson loops themselves have been considered so far.

The SU(2) calculation [5] relied on all Wilson loops up to length 6 as depicted in Fig. 1, and the SU(2) representations $\nu = {}^1/_2$, 1, and ${}^2/_3$ were taken into account. As suggested by lowest order strong coupling (SC) expansion the $\nu \neq {}^1/_2$ representations are suppressed at finite distance. Therefore we have neglected higher representations in subsequent SU(3) investigations [8,9]. In the following we will omit the index ν of $O_{i,\nu}$ if we consider the fundamental representation.

In the continuum limit rotation invariance is supposed to become restored, and the eigenstates of the transfer matrix can be classified according to irreducible representations of the 3-d rotation group. For finite values of β on the lattice we have an exact cubic symmetry, and from the operators $O_{i,\nu}$ of equation (8) we can construct irreducibly representation of the cubic group. In the continuum limit these representations do not uniquely specify the spin, but provide us with selection rules which are of crucial importance. For details cf. section III.a). In section III.b) we construct the irreducible representations of the full cubic group on all Wilson loops up to length 8. The result has already been used and emphasized in Ref. 9,3. In particular for spin J = 0, 1, 2, 3 candidates for all possible P, C = $\pm$ 1 combinations (altogether 16 states) are obtained.

In an MCV calculation one hopes that reasonable large values of β can be reached for which rotation invariance is already approximately true. In the case of SU(2) a different MC investigation [15] has given encouraging results in the accessible scaling region. For the mass gap $m(0^{++})$ it has been first noted in Ref. 8 that the MCV method works surprisingly well in case of the SU(3) gauge group. The computer time needed was much smaller, than one would have expected by a straightforward estimate from previous SU(2) experience. This was conjectured to be related to the large number of statistical variables of a single SU(3) matrix, and an explanation may therefore be connected with the recent results concerning the SU(N), $N \to \infty$ limit [16]. In subsequent MCV investigations [9),10)] the mass gap estimate was slightly improved and results for higher spin SU(3) glueball states were reported. The latter results are quite different from previous SC predictions in a pioneering work by Kogut, Sinclair and Susskind [17].

In chapter IV of this paper we present in detail our MCV calculations on an $4^3 \cdot 8$ lattice, relying on correlations between all Wilson loops up to length 6 (Fig. 1). Due to an enlarged MC statistics our previous results [8),9)] (cf. also [3)]) are improved. Further we present some lowest order spin wave ($\beta \to \infty$) results and compare with old [17]

and new [18) - 21)] SC results. Summary and conclusions are given in chapter V. Finally some technical details are delegated to appendixes: Appendix A explains how the minimization is actually done and Appendix B contains details of the spin wave calculation.

Part II of this paper will contain MCV results on an $5^3 \cdot 8$ lattice, relying on Wilson loops up to length 8.

II. Preliminaries:

In the first part of this chapter we summarize the MC procedure with emphasis on random (R) and systematic (S) upgrading. The second part collects well-known results concerning the symmetry group of the cube. These results are needed in section III.

II.a The Monte Carlo Method

We like to calculate the statistical average $\langle O \rangle$ with respect to a partition function Z, as for instance given by (I.1). The MC technique consists of setting up a Markovian process. At each step a state x of the system is transferred into a new state x' according to a probability matrix $P(x \to x') \geq 0$. In the limit of an infinite number of steps, the arithmetic average over states in this sequence converges against the statistical average $\langle O \rangle$, if the following three conditions are true (for more details cf. the review of Binder [22)]):

II.1. The normalization: $\sum_{x'} P(x \to x') = 1$.

II.2. All configurations can be reached in a finite number of steps.

II.3. The Boltzmann state is an eigenstate with eigenvalue 1:

$$\sum_{x} P(x \to x')\, e^{-S(x)} = e^{-S(x')} .$$

Sufficient (but not necessary) for condition 3. is detailed balance:

$$\frac{P(x \to x')}{P(x' \to x)} = e^{-\{S(x') - S(x)\}} . \qquad \text{(II.1)}$$

Detailed balance does not uniquely fix the MC procedure. For instance one has still a choice between Metropolis or heat bath upgrading. For our SU(3) calculation we use the heat bath method of Pietarinen [23)]. It is not difficult to check detailed balance for the upgrading of a single link. Hence a random choice of a link and subsequent upgrading of this link defines an upgrading matrix, which acts on the

whole system and fulfills detailed balance. Successive applications of this matrix define an upgrading procedure, which we call R-upgrading. Detailed balance remains true, because powers of a matrix preserve detailed balance (use 1.). For R-upgrading we define a sweep by upgrading each link once in the mean. The major part of our results (including [9]) is obtained using R-upgrading.

A more common [24] upgrading procedure - which we call S-upgrading - is to go in a systematic way through the lattice, such that in one sweep each link is upgraded precisely once. The matrix for one sweep defines the Markovian process and is an ordered product of the upgrading matrices for the single links. S-upgrading does not satisfy detailed balance, but condition 3. is still true. For part of our results (including [8]) we have used S-upgrading. On our $4^3 \cdot 8$ lattice the precise procedure was: Starting with the site $(x_1,x_2,x_3,t) = (0,0,0,0)$ we increase t in steps $\Delta t = 1$ up to t = 7 keeping $(x_1,x_2,x_3) = (0,0,0)$ fixed. Then we repeat this keeping $(x_1,x_2,x_3) = (0,0,1)$, up to, (3,3,3) fixed. At each site we upgrade successively the link in t,x_3,x_2, and finally x_1-direction. For mean values of operators, and correlations related to the mass gap we do not note a problem with the convergence of S-upgrading. For a positive definite correlation related to the $m(0^{--})$ glueball we find [9], however, negative values (cf. section IVb, Table 8) with a rather high confidence level. After changing our algorithmen to R-upgrading the phenomenon disappeared immediately. This indicates in case of S-upgrading possible metastable states and a bad convergence for some observables. Independently similar observations have been made in other MC investigations [25].

II.b The Symmetry Group of the Cube

Three dimensional space groups (also called crystal groups) are well-known [26]. Already around 1890 Fedorow and independently Schoenflies enumerated all 230 space groups in three dimensions. Bethe [27] constructed the irreducible representations of crystallographic point groups and considered applications to the splitting of energy levels in crystal fields. Finally the construction of all irreducible representations of the 230 space groups was outlined 1936 by Seitz [28].

We are concerned with the 48 element symmetry group of the cube O_h, which is the direct product of the 24 element cubic group O and the group of order two $\{+1, -1\}$. In contrary to the cubic group O the group O_h contains also reflections. Each of the non-identity elements of the cubic group O can be interpreted as a rotation around an uniquely determined symmetry axis of a cube. The order of an axis is defined to be the number of different rotations (including the identity), which can be performed around this axis. We fix our notation by means of Fig. 2. There are three axis of order four C_4^i (i = 1,2,3), four axis of order three C_3^i (i = 1, ..., 4), and six axis of order two C_2^i (i = 1, ..., 6). Altogether this amounts to $3 \cdot 3 + 4 \cdot 2 + 6 + 1 = 24$ elements. We denote the smallest positive rotation around the axis C_K^i by the same symbol as the axis. There are five classes of conjugate elements: $E = \{1\}$, $C_4 = \{C_4^{(i)}, (C_4^{(i)})^3\}$, $C_4^2 = \{(C_4^i)^2\}$, $C_3 = \{C_3^i, (C_3^i)^2\}$, and $C_2 = \{C_2^i\}$. Hence there are five inequivalent irreducible representations. By the theorem of Burnside the squared dimensions of these representations have to add up to the order of the group (i.e. 24). The only possible dimensions are then 1,1,2,3, and 3. In the notation of crystallographic point groups (cf. Altman [26]) the representations are denoted by A_1, A_2, E, T_1, and T_2. Each representation is up to equivalence fixed by its characters on the classes of conjugate elements as reproduced in Table 1. A_1 is the trivial and T_1 the vector representation.

Including parity is straightforward. The elements g_h of the symmetry group of the cube are of form $g_h = g \times 1$ or $g_h = g \times -1$, $g \in O$. Hence these are ten classes of conjugate elements and ten inequivalent irreducible representations. The representations are denoted by $A_1^{\pm}$, $A_2^{\pm}$, $E^{\pm}$, $T_1^{\pm}$, and $T_2^{\pm}$ according to partiy $P = \pm 1$. If we have (in the corresponding representation) for the character $\chi(g \times 1) = \chi(g \times -1)$ the P = +1 sign stands. Otherwise we have $\chi(g \times 1) = -\chi(g \times -1)$ and the P = -1 sign stands.

In the forthcoming sections we will consider representations, which are defined on operators with a definite C-parity. In that case our complete notation reads:

$$R^{PC} \text{ with } R = A_1, A_2, E, T_1, T_2 \text{ and } P = \pm 1,\ C = \pm 1. \qquad \text{(II.2)}$$

III. Spin on the lattice

In part a) of this chapter we explain the relationship between spin states in the continuum limit of lattice gauge theories and representations of the cubic group. In part b) we construct irreducible representations of the symmetry group of the cube on Wilson loop operators.

III.a Spin states and the cubic group

We assume that the continuum limit of SU(3) lattice gauge theory exists and rotation invariance becomes restored. Then we have in the continuum limit superselection rules according to irreducible representations of the rotation group. States which belong to an irreducible representation D_J of spin J are denoted by

$$|\psi\rangle_J \,, \qquad |\beta = \infty| \,. \tag{III.1}$$

We only consider integer spin J = 0,1, ... For simplicity we also neglect parity and C-parity in the subsequent discussion. The extension is trivial.

For all values of β we have on the hypercubic lattice the exact cubic symmetry. Hence we have superselection rules according to the five irreducible representations of the cubic group O. We now consider states

$$|\psi\rangle_R \qquad (R = A_1, A_2, E, T_1, T_2) \tag{III.2}$$

which belong to an irreducible representation R of the cubic group O. In the continuum limit ($\beta = \infty$) these states can be expanded into states of spin J:

$$|\psi\rangle_R = \sum_{J,m} c^R_{J,m} \, |\psi\rangle_{J,m} \tag{III.3}$$

Of crucial importance is: On the r.h.s. of equation (III.2) spin J can only contribute if

$$D^O_J \supset R \,. \tag{III.4}$$

Here D^O_J is the subduced representation of D_J , which is obtained by trivially embedding the cubic group O into the rotation group.

Up to J = 12 the subduced representations can be read off from the tables of Altmann and Cracknell [29]. For the convenience of the reader we list the result in Table 2. (A recent discussion within lattice gauge theory and a generalization to half-integer spin can be found in Ref. 30.) From Table 2 we note, subduced representations with $J \geq 2$ are reducible, and only up to J = 3 new irreducible representations of the cubic group (A_2 for J = 3) show up.

Let us now consider the variational definition (I.5) of the mass gap and restrict the variation to states

$$|\psi\rangle_R \qquad \text{with} \qquad \langle 0|\psi\rangle_R = 0 \,. \tag{III.5}$$

We denote the corresponding eigenvalues by m(R) and make for the continuum limit the assumption:

The eigenvalue m(R) corresponds to the lowest allowed spin in the sector $|\psi\rangle_R$.

Then Table 2 gives us the following results ($\beta = \infty$):

$$m(0^{PC}) = m(A_1^{PC}) \tag{III.6a}$$

$$m(1^{PC}) = m(T_1^{PC}) \tag{III.6b}$$

$$m(2^{PC}) = m(E^{PC}) = m\,(T_2^{PC}) \tag{III.6c}$$

$$m(3^{PC}) = m(A_2^{PC}) \tag{III.6d}$$

For completeness we have included P- and C-parity. Accepting $m(2^{PC}) < m(4^{PC})$, equation (III.6c) is a consistency condition for $m(2^{PC}) < m(3^{PC})$. Another consistency check is

$$m(T_1^{PC}) < m(A_2^{PC}) \qquad \text{(III.7)}$$

for the assumption $m(1^{PC}) < m(3^{PC})$. For the important trajectories $J = 0,2, \ldots$ and $J = 1,3, \ldots$ our assumption would follow from a Regge picture. Let us note: Even if the assumption would fail, one could still obtain reasonable results. For instance if $m(A_2^{PC}) = m(T_2^{PC}) < m(E^{PC})$ one would conclude that the spin 3^{PC} state is lower than the 2^{PC} state.

We are interested in an MCV calculation at finite β. Encouraged by the MC results of Ref. 15, the hope is to come into a region of β, where equations (III.6) hold in an approximate sense. As far as we are limited to estimate (in a given sector $|\Psi\rangle_R$) only the lowest energy eigenvalue above the vacuum, we can only consider spin $J \leq 3$. Details of our MCV investigation are presented in part IV.. Concerning the assumption above we find a posteriori reasonable consistency with our MCV results.

III.b Irreducible representations of the Cubic Group on Wilson Loops

We construct all irreducible representations of the symmetry group of the cube O_h on spacelike Wilson loop operators (I.8) up to length 8. Prototyps of Wilson loops (by this we mean Wilson loops of different shape) up to length 6 are depicted in Fig. 1 (sectionI) and of length 8 in Fig. 3.

For SU(N) with $N \geq 3$ the characters are complex, and the Wilson loops have an orientation, defined by the order in the product of U-matrices: Regard the formula for the first Wilson loop in Fig. 4. In the continuum Lagrangian we have under C-parity

$$A_\mu \xrightarrow{C} -A_\mu^T \qquad \text{(III.8)}$$

for a Hermitian choice of the gauge field A_μ. It follows the simple rule:

Real parts of Wilson loop operators have C-parity C = + 1, imaginary parts have C-parity C = 1 .

Let us consider spacelike Wilson loop operators $O_{i,\nu}$ of length L, as defined by equation (I.8). For our forthcoming consideration only the shape and the orientation of the associated path C_i is important, which can be represented by an L-tupel:

$$(\hat{f}_1, \ldots, \hat{f}_L) \quad \text{with} \quad \sum_{\lambda=1}^{L} \hat{f}_\lambda = 0 \; . \qquad \text{(III.9)}$$

Here the vectors $\hat{f}_i$ are $\hat{f}_i \in \{\pm \hat{e}_j \mid j = 1,2,3\}$, where $\hat{e}_j$ are the unit vectors corresponding to the spacelike coordinates of our lattice. For instance the sum corresponding to the first Wilson loop of Fig. 4 may be given by $(\hat{e}_2, \hat{e}_3, -\hat{e}_2, -\hat{e}_3)$, and if we reverse the orientation it becomes $(\hat{e}_3, \hat{e}_2, -\hat{e}_3, -\hat{e}_2)$. Two L-tupels are called equivalent, if they are identical up to cyclic permutation. The equivalence class corresponding to $(\hat{f}_1, \ldots, \hat{f}_L)$ is denoted by $[\hat{f}_1, \ldots, \hat{f}_L]$.

Under C-parity we have

$$C[\hat{f}_1, \ldots, \hat{f}_L] = [-\hat{f}_L, -\hat{f}_{L-1}, \ldots, -\hat{f}_1] \; . \qquad \text{(III.10)}$$

We now consider C = $\pm$ operators $O^{\pm}_{i,\nu}$, defined by the combinations

$$[\hat{f}_1, \ldots, \hat{f}_L]_\pm = [\hat{f}_1, \ldots, \hat{f}_L] \pm [-\hat{f}_L, \ldots, -\hat{f}_1] \qquad \text{(III.11)}$$

On $O^{\pm}_{i,\nu}$ operators of fixed shape we generate a representation $\mathfrak{M}$ of O_h by means of

$$\mathfrak{M}_g [\hat{f}_1, \ldots, \hat{f}_L]_\pm \overset{\text{def}}{=} [M_g \hat{f}_1, \ldots, M_g \hat{f}_L] \qquad \text{(III.12)}$$

for $g \in O_h$, and M_g being the matrix corresponding to g in the vector representation on the basis $\hat{e}_i$ $(i = 1,2,3)$.

Including C-parity the dimension d of the generated representation is less or equal 96 ($96 = 2 \cdot 48$, 48 = order of O_h). The d x d representation matrix $\mathfrak{M}_g$ consists of elements $(\mathfrak{M}_g)_{ij}$ which are ± 1 or zero. In Fig. 4 we have listed (up to opposite orientation) all Wilson loops which are generated from prototyps of Wilson loops up to length 6 (Fig. 1). The dimensions of the representations are d = 6 for the plaquettes, d = 12 for the double plaquettes, d = 24 for the bent plaquettes, and d = 8 for the twisted plaquettes.

The irreducible contents of the representation $\mathfrak{M}$ is best explored by means of the character relation. For fixed C-parity (C = + 1 or C = - 1) the multiplicity m_R^P of the representation R^P in the decomposition of $\mathfrak{M}$ into irreducible representations is given by

$$m_R^P = \frac{1}{48} \sum_K n_K \chi_K^{\mathfrak{M}} \chi_K^{R^P} . \qquad \text{(III.13)}$$

The sum goes over all classes of conjugate elements, and n_K is the number of elements in class K. In our calculation we have taken the trace of one matrix representative in each conjugacy class of the representation $\mathfrak{M}$, and the irreducible characters $\chi_K^{R^P}$ where taken from a table (which is easily obtained from Table 1). For Wilson loops up to length 6 (numeration as in Fig. 1) our results are given in Table 3.1 and for Wilson loops of length 8 (numeration as in Fig. 3) our results are given in Table 3.2. The results for SU(2) are simply obtained by omitting the C = - 1 contributions, and by taking $\frac{1}{2}$d as dimension for the corresponding representation $\mathfrak{M}$ on SU(2) Wilson loops.

A notable result from Tables 3 is that from Wilson loops up to length 8 candidates for all possible J^{PC} states with P = $\pm$, C = $\pm$ and J = 0,1,2,3 (i.e. altogether 16 states) can be constructed. Of particular importance are so called "oddballs" [31]. Oddballs are glueballs with a J^{PC} combination, which is not allowed as $q\bar{q}$ flavour

singlet state in the quark model. Therefore (ignoring in some cases exotic states) the (at present with MC methods hardly attackable) mixing problem does not exist. Our classification involves only basic principles of lattice gauge theory. However, no dynamic information is obtained so far and we do not know whether in the continuum limit all possible 16 states are realized in the spectrum of physical states.

For carrying out an MCV calculation, the information contained in Tables 3 is insufficient. For each irreducible representation we have to calculate explicitely an orthonormal basis. In principle this could be done by using well-known projector methods (cf. e.g. 30)). For large dimensional representations this is, however, rather clumsy and in practice a different method (cf. Altmann 26)) has turned out to be useful. The method relies on an elaboration of Shur's lemma: Let C be a matrix which commutes with $\mathfrak{M}$ (i.e. all matrices of the representation $\mathfrak{M} = \{\mathfrak{M}_g\}$) and let A be the matrix which diagonalizes C (ACA^{-1} = diagonal), then A reduces (not necessarily completely) the representation $\mathfrak{M}$, and in the next step one may go on with the representation

$$A\mathfrak{M}A^{-1} = \{A\mathfrak{M}_g A^{-1} \mid \mathfrak{M}_g \in \mathfrak{M}\} .$$

Matrices C, which commute with $\mathfrak{M}$, can be constructed by summing the matrices of a conjugacy class of $\mathfrak{M}$. It has turned out that we were able to reduce completely all our considered representations, invoking only a few conjugacy classes in each case.

For later minimization it is important, to construct for different operators irreducible representations, which behave exactly the same under the cubic group. This was done by proceeding with a projector method.

For Wilson loops up to length 6 orthonormal basis systems (as used in our MCV calculation) are given in the Tables 4.1 - 4.4. The notation for the operators is fixed by means of Fig. 4. We have also calculated the analog results for all Wilson loops of length 8. The expressions are very lengthy and unsuitable for publication. Interested readers can obtain the complete result from the authors.

IV. The Monte Carlo Results

IV.a Monte Carlo Calculations and the Continuum Limit

The aim of our MCV calculation is to obtain results, which can be extrapolated to the continuum limit $\beta \to \infty$. Let us consider a mass eigenvalue $m(J^{PC})$. If in a MC investigation we find a scaling window $\beta_1 \leq \beta \leq \beta_2$, where $m(J^{PC})$ scales approximately according to the asymptotic renormalization group prediction (I.4), we feel free to extrapolate all the way to the continuum limit. There are of course various pitfalls. For instance a singularity in the complex β-plane may simulate a scaling window without being connected to the asymptotic behaviour. Also higher order corrections to Λ^L (I.2) can hardly be seen in a small scaling window, but may significantly change the final value. The best way to feel free from these pitfalls would be to enlarge the scaling window and to establish to a certain extend universality. This does, however, go beyond the scope of the present investigation.

In our opinion the existence of a scaling window is a minimal requirement for argueing about a connection with the continuum limit. There are no simple rules, which quarantee one to find a scaling window within a MC calculation. Even without changing Λ^L it is easily possible (for instance by introducing a constraint $\mathrm{Tr}(1 - \mathcal{U}(\beta)) < \varepsilon$) to shift the scaling region to such a large correlation length $\xi = 1/m_g$, that it cannot be reached within nowadays conventional MC methods. On the other hand the often quoted necessary condition $a \ll \xi \ll L$ has turned out to be too restrictive. Using the Wilson action, SU(2) [5,3] and SU(3) [8] mass gap estimates exhibit a scaling window for $\xi \lesssim a$. Heuristic arguments [3] indicate that an improved condition is

$$a \ll \xi_r \ll L. \qquad \text{(IV.1)}$$

Here ξ_r is the "relevant range of interaction" and of order $\xi_r \simeq d \cdot \xi$ in d dimensions. For higher masses a similar behaviour may hold, if one replaces ξ by the corresponding new inverse mass. Therefore for larger mass values the onset of scaling is argued to be shifted to a higher value β_1.

IV.b The Mass Gap

We present results of MC simulations with R-upgrading on an $4^3 \cdot 8$ lattice. We measure Wilson loops O_i ($i = 1, \ldots, 4$) up to length 6 (as given in Fig. 1 and 4) in the fundamental representation. Together with the number of performed sweeps their expectation values are given in Table 5. The mean values are obtained from the whole statistics, and error bars are calculated by dividing the whole set of measurements into 14 subsamples. For each β value, we used as starting point the last configuration generated by our previous S-upgrade runs [8], and the upgrading of a single link variable (SU(3) matrix) was done with Pietarinen's [23] heat bath method. The used computer time was about 80h CDC 7600. We have also included the first operator of length 8 (Fig. 3) in our measurements on the $4^3 \cdot 8$ lattice. Because of finite size effects we do not include these results in this part of the paper.

In Fig. 5a and 5b we present graphically the mean values of the operators and their derivatives. The derivatives and their error bars are calculated from the next nearest neighbours and their error bars. The lines are mean square fits to the data and only intended to guide the eyes. All derivatives have a rather pronounced peak in the region $\beta \approx 5.6 - 5.7$.

To perform our $m_g = m(0^{++})$ mass gap estimate we construct for each of the operators O_i the 1-d irreducible representation A_1: $O_i^{A_1}$. The index A_1 is suppressed in the following. Concerning the minimization procedure we follow our previous work [5]. We consider truncated correlation functions

$$C_{\hat{\imath}\hat{\jmath}}(t) = \langle 0 | O_{\hat{\imath}}(0)\, O_{\hat{\jmath}}(t) | 0 \rangle - \langle 0 | O_{\hat{\imath}} | 0 \rangle \langle 0 | O_{\hat{\jmath}} | 0 \rangle \qquad (t = 1, 2, \ldots). \qquad \text{(IV.2)}$$

For single operators O_i we define glueball masses

$$m_{\hat{\imath}}(t) = \frac{-1}{t} \ln \left(\frac{C_{\hat{\imath}\hat{\imath}}(t)}{C_{\hat{\imath}\hat{\imath}}(0)} \right) \qquad (t = 1, 2, \ldots) \qquad \text{(IV.3a)}$$

and

$$\hat{m}_\lambda(t) = -\ln\left(\frac{C_{\lambda\lambda}(t)}{C_{\lambda\lambda}(t-1)}\right) \qquad (t=1,2,\ldots) \,. \tag{IV.3b}$$

The variational principle leads to the equation

$$m_g(t) = -\frac{1}{t}\ln\left(\max_{\{c_i\}}\frac{\sum_{\lambda\lambda'} c_\lambda c_{\lambda'} C_{\lambda\lambda'}(t)}{\sum_{\lambda\lambda'} c_\lambda c_{\lambda'} C_{\lambda\lambda'}(0)}\right). \tag{IV.4}$$

Because of the bias [5] minimization at a distance $t > 1$ is only possible for an exceptionally large statistics (cf. also Ref. (5, addendum)). In practice the coefficients $\{c_i\}$ are calculated by converting equation (IV.4) into an eigenvalue problem (cf. Appendix A). In the following we work with wave functions, which are determined from correlations at distances t = 1. Let

$$\mathcal{O} = \sum_\lambda c_\lambda \mathcal{O}_\lambda \tag{IV.5a}$$

be the corresponding operator. Its correlation function is

$$C(t) = \langle 0|\mathcal{O}(0)\,\mathcal{O}(t)|0\rangle - \langle 0|\mathcal{O}|0\rangle^2 \tag{IV.5b}$$

We define again glueball masses, denoted $m_g(t)$ and $\hat{m}_g(t)$, by means of equations (IV.3) with C_{ii} replaced by C. Equation (IV.3b) gives of course better (lower) values than equation (IV.3a), but leads to t-times bigger error bars. Our MC statistics is, however, sufficient for using $\hat{m}_g(t)$ at distance t = 2.

Fig. 6a shows $\hat{m}_1(t)$, (t = 1,2) as function of β and Fig. 6b gives the results $\hat{m}_g(t)$, (t = 1,2) after minimization. The three solid lines in each figure follow the asymptotic renormalization group

prediction (I.2,4) and represent our final mass gap estimate. The broken lines on the l.h. sides are the SC expansion to order β. For the plaquette correlations we have also calculated to lowest order the asymptotic behaviour $\beta \to \infty$ (cf. Appendix B). This is the spin wave region. The resulting values for $\hat{m}_1(t)$, (t = 1,2) on an $4^3 \cdot 8$ lattice are the broken lines on the r.h. side of Fig. 6a.

Within a scaling window $5.1 \lesssim \beta \lesssim 5.6$ already the results from distance t = 1 follow remarkable well the asymptotic scaling curve. Within error bars we find agreement with our S-upgrading results [8]. As compared with $m_1(1)$, the whole curve for $m_g(1)$ is considerably lowered as consequence of minimization. This means scaling alone does not guarantee stable extrapolations. A second look at both curves exhibits a suspicious overshooting of scaling, in particular for the curve after minimization. Possible explanations are at hand:

1. A nearby singularity in the complex β-plane could be responsible [32].
2. There may be large next order perturbative corrections to Λ^L as defined by (I.2) [33].
3. Finite size effects due to the small spacelike extend of our lattice are expected [34].

Our data on the larger $5^3 \cdot 8$ lattice support 3..

In Table 6 we collect our final results for $m_i(1)$ (i = 1, ..., 4), $m_g(1)$, $m_g(2)$ and $\hat{m}_g(2)$. A remarkable feature of the data $m_i(1)$ (i = 1, ..., 4) is the fact that all operators considered lead to very similar mass gap estimates. The best (lowest) values are obtained from operator # 3. In contrast we have in the SC limit $\beta \to 0$

$$m_1(1) = 4\ln(1/\beta) + \mathcal{O}(1)$$

whereas

$$m_3(1) = 6\ln(1/\beta) + \mathcal{O}(1)$$

The fact that $m_1(1) \approx m_3(1)$ in the scaling region, is an example how some kind of continuum like behaviour for large distances is obtained just after the crossover region already at small distances.

Table 7 contains for each β value the wave function, as used for calculating $m_g(t)$ and $\hat{m}_g(t)$. As previously all error bars are with respect to 14 subsamples. If the mean value from all data differs from the mean value of the mean values of the subsamples, we have a signal for a bias. In that way the bias [5] from the minimization procedure as well as the bias in the correlation functions is estimated to be much smaller than the given error bars.

Looking at Fig. 6b we find our scaling curve from $m_g(1)$ considerably lowered by the results from distance t = 2. Results from distance t = 3, which are not represented here because our statistics is insufficient for estimating reliable error bars, indicate a further decreasing tendency. We find, however, that $\hat{m}_g(2)$ agrees well with the values $\hat{m}_i(2)$, (i = 1, ..., 4) (cf. Fig. 6a for $\hat{m}_1(2)$). This fact is an indication that the t = 2 results are already asymptotic. In view of expected finite size effects 3., one should therefore not take very low values too seriously. We are thus led to the estimate

$$m(0^{++}) = (280 \pm 50)\, \Lambda^L \qquad \text{(IV.6)}$$

To extract a value in physical units, one relies best on MC calculations [35),23)] for the SU(3) string tension, because the experimental determination of Λ^L (I.3) is very crude. The MC calculations give

$$\Lambda^L = (6 \pm 1) \cdot 10^{-3} \sqrt{K}$$

Together with $\sqrt{K} \approx 440$ MeV*) this leads to the order of magnitude

$$m(0^{++}) \approx 750 \text{ Mev.} \qquad \text{(IV.7)}$$

*) This value comes from the Regge slope and is in agreement with the less accurate value (I.3).

In Fig. 6 our scaling window ends drastically at $5.6 < \beta_2 < 5.7$. In contrast to this the scaling window for the string tension [35),23)] extends to a much higher value β_2. This is argued [5] to be due to different spin wave behaviour $\beta \to \infty$ for finite size string tension [36)] and finite size glueball mass (IV.3) definitions. The spin wave result for the SU(3) plaquette operator is calculated in Appendix B. As illustrated in Fig. 6a these results are much higher than values in the scaling window region. It would be interesting to calculate the next perturbative order and to obtain similar results for the other considered operators.

Finally in this section we remark, that SC calculations [18)-21)] lead to SU(3) mass gap estimates, which are in good agreement with the value (IV.6). In particular, as for the string tension [37)], the simple method of taking the asymptotic scaling behaviour as tangent to the last order SC expansion ("tangent method") gives a good result:

$$m(0^{++}) \approx 310\, \Lambda^L . \qquad \text{(IV.9)}$$

The expansion is taken in terms of SU(3) characters.

The SC expansion is done for momentum zero plaquette-plaquette correlations in the A_1 representation. The limit $t \to \infty$ is considered and the available order [18)-20)] is $O(\beta^8)$. It has been shown [5] that a short $t \to \infty$ series agrees (up to the same order) with the series for a fixed small distance t. In the present case presumably t = 3.

IV.c Excited Spin States

Excited spin states where first investigated by Kogut, Sinclair and Susskind [17)], who did an $O(\beta^8)$ SC expansion in the Hamiltonian formulation. Their series is for momentum zero plaquette-plaquette correlations. Extrapolating mass ratios to $\beta \to \infty$ by means of diagonal Padé approximants gives

$$m(1^{+-}) \approx 1.6\, m(0^{++}) \qquad \text{(IV.10a)}$$

and

$$m(2^{++}) \approx 1.0\, m(0^{++}) . \qquad \text{(IV.10b)}$$

An analysis [21] of the analog Euclidean $O(\beta^8)$ SC series [18)-20] agrees well with this order of magnitude. Thus universality seems to be confirmed. We will, however, find disagreement with our MCV results.

Using the results of chapter III, we have built the (connected) correlation functions of all the irreducible operators contained in length 4 and 6 Wilson loops:

$$C^{R^{PC}}_{i_\lambda i_\lambda, m}(t) \qquad (i_\lambda = 1, \ldots, 4).$$

Here m is the "magnetic" quantum number. (m takes 1 value for A_i (i = 1,2) representations, 2 values for the E representation, and 3 values for T_i (i = 1,2) representations.) By construction all representations with the same value of R^{PC} transform identically under the group O_h. Up to statistical fluctuations $C^{R^{PC}}_{ij,m}$ is independent of m. To gain statistics we have considered the scalar correlations

$$C^{R^{PC}}_{i_\lambda i_\lambda}(t) = \sum_m C^{R^{PC}}_{i_\lambda i_\lambda, m}(t) \qquad \text{(IV.11)}$$

Finite distance glueball masses

$$m^{R^{PC}}_{i_\lambda}(t), \quad \hat{m}^{R^{PC}}_{i_\lambda}(t), \quad m^{R^{PC}}(t), \quad \hat{m}^{R^{PC}}(t) \qquad \text{(IV.12)}$$

are defined as in the previous section, cf. equations (IV.3). C_{ii} is replaced by $C^{R^{PC}}_{ii}$ for single operators, and C (IV.5b) is replaced by $C^{R^{PC}}$ in case of minimization.

From Wilson loops up to length 6 we construct candidates for 9 different spin excitation ($\neq 0^{++}$). Our data for these excited

glueball masses are much higher than the corresponding data for $m(0^{++})$. Therefore the results at distance t = 2 are already mainly noise. For selected values of β the results at distance t = 1 are given in Table 8. MC statistics and error estimate are as in the previous section. The bias brought by the minimization procedure is estimated to be less than 10% in all cases. In Table 9 we compare correlations for the 0^{--} state, which were obtained using S-upgrading, with the corresponding R-upgrading correlations. This and similar results convinced us to turn to the R-upgrading procedure.

All our data for excited glueball masses show roughly constant behaviour with β, this means no sign of scaling. Of particular interest is the 2^{++} glueball, because of the SC prediction (IV.10b). Our data for the mass of the 2^{++} glueball as extracted from the plaquette operator (E^{++} representation) and after minimization (over all operators contributing to the E^{++} representation) are shown in Fig. 7. On the l.h. side the SC expansion to order β is indicated. In the spin wave ($\beta \to \infty$) limit the quantity $m_1^{E^{++}}(t)$ has the virtue to be easily evaluated (see Appendix B), and the result for $m_1^{E^{++}}(t)$ on the $4^3 \cdot 8$ lattice is indicated on the r.h. side of Fig. 7. Already for $\beta = 5.0$, $m_1^{E^{++}}(1)$ is very close to it's spin wave limit, and there is no signal for scaling in the whole considered range of β values. Minimization lowers the values slightly, but does not give rise to any drastic changes. Even much higher than $m_1^{E^{++}}(1)$ is $m_1^{T_1^{+-}}(1)$, and the same is true after minimization. For comparing with $m(0^{++})$ we give in Table 10 the fractions $m_1^{E^{++}}(1)/m_1^{A_1^{++}}(1)$ and $m_1^{T_1^{+-}}(1)/m_1^{A_1^{++}}(1)$. Despite the lack of scaling, the values for $m^{E^{++}}(1)$ are nevertheless the lowest obtained mass estimates among all considered representations.

In the continuum limit we expect a cut at $2m(0^{++})$ in the 0^{++} and in the 2^{++} channel. For $J \leq 3$ no other cuts can be made from two 0^{++} states. An excited 0^{++*} state or the 2^{++} state would become unstable if their mass is larger than $2m(0^{++})$. On the lattice a cut becomes a series of poles. As long as we do not analyse our wave function with respect to partial waves, we are not able to distinguish these poles from a bound state with mass larger than $2m(0^{++})$. Typically a cut seen in this way in a MCV calculation should give rise to an

effective mass $> 2m(0^{++})$, because several poles may mix into the wave function. Searching with large MC statistics for an SU(2) $m(0^{++*})$ state ([5], addendum) we found a signal, which was interpreted as a cut. The behaviour of the $m(2^{++})$ state as discussed in this paper is rather similar.

Our MCV results rule out the SC prediction (IV.10b) for the $m(2^{++})$ state. If SC were correct one could not understand, why there is a perfect scaling window for the $m(0^{++})$ state, but no signal for scaling of the $m(2^{++})$ state. If one considers without further analysis the SC series [18),19)] for the $m(0^{++})$ and the $m(2^{++})$ state, one finds $m(2^{++})$ clearly higher than $m(0^{++})$ in the region ($\beta \approx 5.0$), where the SC expansion start to break down. Therefore our results are in contradiction with the continuum extrapolations [17),21)], but not with the SC series [18),19)] itself. Using diagonal Padé approximants, these continuum extrapolations assume the existence of the $m(2^{++})$ state in the continuum spectrum, i.e. $m(2^{++})/m(0^{++}) \to$ const. for $\beta \to \infty$. The MCV calculation has the chance to be selfconsistent with respect to this point. As we find no scaling window for the $m(2^{++})$ state, we have no signal for the existence of this state in the physical continuum spectrum.

The same holds (we obtain only even higher mass values) for the other 8 considered candidates for excited glueball states. Remarkably the obtained values are even higher, than the extrapolation of the lowest order SC series into the considered β region. We interpret these results as a signal for the non-existence of all these states, and the naive prejudices on the spectrum, as gained from bag models [38)] and phenomenological relativistic potential models [31)] may very well be wrong. On the other hand we cannot exclude rather high masses, which should shift scaling to larger β values. (A MCV check of the relativistic energy momentum dispersion could test the extension of the accessible mass range.) Also be rotational nature of excited glueball states could be an obstacle to early scaling. This criticism would as well apply to the available SC expansions. The scaling region for excited states may then be totally out of present computer and SC possibilities, at least within the conventional methods discussed here.

V. Summary and Conclusions

In chapter III we have worked out the relation between irreducible representations of the cubic group on lattice wave functions and spin J states in the continuum limit. For Wilson loops up to length 8 we have constructed all irreducible representations of the full cubic group. Candidates for 16 different spin states in the continuum limit are obtained:

$$J^{PC}, \ (J = 0,1,2,3), \quad P = \pm, \quad C = \pm. \tag{V.1}$$

Our MC results are contained in chapter IV. In section IV.b we find a clear scaling window for the $m(0^{++})$ state. This leads to the estimate

$$m(0^{++}) = (280 \pm 50)\,\Lambda^{L} \approx 750 \text{ Mev}, \tag{V.2}$$

in good agreement with SC results [18)-21)].

The situation is quite different for excited spin states considered in section IV.c. We investigate (in part I of this paper) the 9 states ($J^{PC} \neq 0^{++}$), which can be constructed (Table 3) from Wilson loops up to length 6, and find no scaling window for any of these states. Therefore we have no signal for the existence of any of these states in the physical spectrum.

By assuming the existence of such states in the continuum limit, SC predictions [17),21)] (equations (IV.10)) for low lying 1^{+-} and 2^{++} states are obtained. At least the mass prediction for 2^{++} (IV.10b) is ruled out by the present MCV investigation. We can of course not exclude that the scaling region for excited glueball states cannot be reached in our MCV investigation. But such a criticism would also apply to the existing SC predictions.

In conclusion we find clear evidence for the existence of an 0^{++} state and no evidence for the existence of any other state.

References

1. H. Fritzsch and M. Gell-Mann, Proc. XVI Int. Conf. High Energy Physics, Vol. 2 (Chicago 1972).
   See also H. Fritzsch and P. Minkowski, Nuovo Cimento 30A (1975) 393.
2. K. Wilson, Cargèse lectures 1979, edited by G. 't Hooft et al., Plenum Press, New York, 1980;
   M. Creutz, L. Jacobs and C. Rebbi, Phys. Rev. D20 (1979) 1915;
   M. Creutz, Phys. Rev. D21 (1980) 2308.
3. For a review see: B. Berg, Preprint, CERN TH.3327.
   Since this review was completed, several new investigations have been carried out. See Ref. 39.
4. The MCV method as used in Ref. 5) - 10) has been suggested by K. Wilson, Abingdon Meeting on Lattice Gauge Theories (1981).
5. B. Berg, A. Billoire and C. Rebbi, Annal. Phys. (NY) 142 (1982) 185 and addendum, to be published.
6. M. Falcioni, E. Marinari, M.L. Paciello, G. Parisi, R. Rapuano, B. Taglienti and Zhang-Yi-cheng, Phys. Lett. 110B (1982) 295.
7. K. Ishikawa, M. Teper and G. Schierholz, Phys. Lett. 110B (1982) 399.
8. B. Berg and A. Billoire, Phys. Lett. 113B (1982) 65.
9. B. Berg and A. Billoire, Phys. Lett. 114B (1982) 324.
10. K. Ishikawa, M. Teper and G. Schierholz, Phys. Lett. 116B (1982) 429 and Preprint DESY 82-53.
11. A. Hurwitz, Nachr. Gött. Ges. Wissensch. 1897, p. 71;
    I. Shur, Sitzungsber. Preuss. Akad. 1924, pp. 189, 297, 346;
    A. Haar, Ann. Math. 34 (1933) 147.
12. A. Hasenfratz and P. Hasenfratz, Nucl. Phys. B193 (1981) 210, and references therein.

13. A.J. Buras p. 636 ff. in "Proceedings of the 1981 International Symposium on Lepton and Photon Interactions at High Energies". (Editor: W. Pfeil, Physikalisches Institut, University of Bonn). We have taken the lower range of values $\Lambda_{\overline{MS}} \approx 160 \pm^{100}_{80}$ Mev) as given by the author.
14. M. Creutz, Phys.Rev. D15 (1977) 1128;
    M. Lüscher, Commun. Math. Phys. 54 (1977) 283;
    K. Osterwalder and E. Seiler, Ann. Phys. (N.Y.) 110 (1978) 440.
15. C.B. Lang and C. Rebbi, Phys. Lett. 115B (1982) 137.
16. T. Eguchi and H. Kawai, Phys. Rev. Lett. 48 (1982) 1063;
    G. Bhanot, U.M. Heller and H. Neuberger, Phys. Lett. 113B (1982) 47;
    G. Parisi, Phys. Lett. 112B (1982) 463;
    D.J. Gross and Y. Kitazawa, Princeton preprint (1982).
    S.R. Das and S.R. Wadia, Preprint, EFI 82-15 (1982)
17. J. Kogut, D.K. Sinclair and L. Susskind, Nucl. Phys. B114 (1976) 199.
18. G. Münster, Nucl. Phys. B190 [FS3] (1981) 439, Erratum B200 [FS4] (1982) 536, and 2. Erratum B205 FS5 (1982) 545. There exist also unpublished results of Münster for spin 1 and spin 2 states.
19. K. Seo, Nucl. Phys. B (to be published).
20. N. Kimura and A. Ukawa, unpublished.
21. J. Smit, Preprint ITFA-82-3 (1982);
    G. Münster, Preprint, BERN, BUTP-21 (1982).
22. K. Binder, in Phase Transitions and Critical Pehnomena, eds. C. Domb and M.S. Green, Vol. 5 (Academic Press, New York, 1976).
23. E. Pietarinen, Nucl. Phys. B190 [FS3] (1981) 349.
24. Cf. e.g. Creutz et al. Ref. 2.
25. S.J. Anthony, C.H. Llewellyn Smith, J.F. Wheater, Phys. Lett. 116B (1982) 287;
    C. Michael (private communication).

26. For an introduction see:
S.L. Altmann in D.R. Bates (ed.) "Quantum Theory II", Academic Press 1962;
G.J. Ljubarski, "Anwendungen der Gruppentheorie in der Physik", VEB Deutscher Verlag der Wissenschaften.

27. H. Bethe, Ann. der Physik 3 (1929) 133.

28. F. Seitz, Ann. Math. 37 (1936) 17.

29. S.L. Altmann and A.P. Cracknell, Rev. Mod. Phys. 37 (1965) 19.

30. R.C. Johnson, Phys. Lett. 114B (1982) 147.

31. For a recent status report cf. S. Meshkov, Proceedings of the JOHNS HOPKINS Workshop on Current Problems in Particle Theory 6, (Florence 1982), pp. 185.

32. Such a singularity is indicated by the peak in the specific heat:

B. Lautrup and M. Nauenberg, Phys. Rev. Lett. 45 (1981) 1755;
M. Falcioni, E. Marinari, M.L. Paciello, G. Parisi and B. Taglienti, Phys. Lett. 102B (1981) 270 and
Nucl. Phys. B190 [FS3] (1981) 782.

For SU(2) consistency with the asymptotic scaling behaviour (I.2) has been shown:
M. Nauenberg, T. Schalk and R. Brower, Phys. Rev. D24 (1981) 548.

33. Such corrections are conjectured to be responsible for scaling deviations in the 2-d σ -model:
G. Martinelli, G. Parisi and R, Petronzio, Phys. Lett. 100B (1981) 485:
B. Berg and M. Lüscher, Nucl. Phys. B190 [FS3] (1981) 412.

34. Shrinking the size in time direction leads to the well-known deconfining phase transition (and massless particles):

J. Kuti, J. Polónyi and K. Szláchanyi, Phys. Lett. 98B (1981) 199;
L. McLerran and B. Svetitsky, Phys. Lett. 98B (1981) 195;
J. Engels, F. Karsch, H. Satz and I. Montvay, Phys. Lett. 101B (1981) 89;
K. Kajantie, C. Montonen and E. Pietarinen, Z.Phys. C9 (1981) 253.

35. M. Creutz, Phys. Rev. Lett 45 (1980) 313;
M. Creutz and K.J.M. Moriaty, Phys. Rev. D26 (1982) 2166.

36. T. Hattori and H. Kawai, Phys. Lett. 105B (1981) 43;
J.P. Kovall and H. Neuberger, Univ. California, Berkeley, preprint, 1981.

37. G. Münster, Phys. Lett. B95 (1980) 59;
G. Münster and P. Weisz, Phys. Lett. B96 (1980) 119.

38. For a review see:
P. Hasenfratz and J. Kuti, Phys. Reports 40C (1978) 75.

39. M. Falcioni, E. Marinari, M.L. Paciello, G. Parisi, B. Taglienti and Zhang-Yi-cheng, Preprint, Roma (August 1982) (to be pubished in Nucl. Phys. B.);
C. Michael and I. Teasdale, Preprint, Liverpool LTH 96 (August 1982);
K.H. Mütter and K. Schilling, Preprint, Wuppertal WU B 82-14 (September 1982).

Recently we got aware of another early lattice calculation:
W.A. Bardeen, R.B. Pearson and E. Rabinovici, Phys. Rev. D21, (1980) 1037.

Acknowledgements

We would like to thank P. Hasenfratz for useful discussion, and R. Petronzio for organizing generous support with computer time. Most of the computer calculations were carried out at the CERN CDC 7600.

Appendix A The Minimization

We want to determine the set of coefficient $\{c_i\}$ which maximize the expression

$$\frac{\sum_{\lambda\gamma} c_\lambda c_\gamma C_{\lambda\gamma}(t_1)}{\sum_{\lambda\gamma} c_\lambda c_\gamma C_{\lambda\gamma}(t_2)} \quad , \quad (t_1 > t_2) \qquad \text{(A.1)}$$

This is best done by transforming this problem into the eigenvalue problem (Recall that the matrix C_{ij} is symmetric)

$$\sum_\gamma C_{\lambda\gamma}(t_1)\, c_\gamma = \lambda \sum_\gamma C_{\lambda\gamma}(t_2)\, c_\gamma \quad , \qquad \text{(A.2)}$$

whose eigenvalue are precisely the extrema of (A.1). It is easy to show that equation (A.2) has only real eigenvalues, except when the expressions $\sum c_i C_{ij}(t_1) c_j$ and $\sum c_i C_{ij}(t_2) c_j$ have zeros. This happens when the statistics is not good enough.

Appendix B Spin wave analysis

The generalization of the result of Ref. 5 to SU(N) is

$$C_{11}(t) = 3 N_s^3 \langle \sigma_1(0)\, \sigma_1(t) \rangle_c$$

$$= \frac{N^2-1}{3 N_s^3 N_t^2 \beta^2} \sum_{\substack{\vec{n} n_4 K_4 \\ (\vec{n}, n_4) \neq 0 \\ (\vec{n}, K_4) \neq 0}} \frac{\cos(n_4 t)\cos(K_4 t)\, \pi(\vec{n}, 0)^2}{\pi(\vec{n}, n_4)\, \pi(\vec{n}, K_4)}$$

$$\sigma_1(t) = \frac{1}{3 N_s^3} \sum_{\substack{\vec{x} \\ \text{orientations}}} \mathrm{Re}\left[\frac{1}{N} \mathrm{Tr}\, U(\vec{x}, t)\right]$$

$$\pi(\vec{n}, n_4) = \sum_{\mu=1}^{4} (1 - \cos n_\mu)$$

Numerical results for the quantities $m_1(t)$ and $\hat{m}_1(t)$ for an $4^3 \cdot 8$ lattice can be found in Table 11. Note the paradoxal nearly exponantial behaviour of correlation functions at small t. It is however easy to show that, on an infinite lattice, correlation functions have the expected power law fall off

$$C_{11}(t) \underset{t\to\infty}{\sim} \frac{N^2-1}{(2\pi)^2} \frac{5}{2\beta^2 t^5}$$

The above results can be readily extended to the correlation function of the E^{++} operator built from one-plaquette Wilson loops

$$C_{11}(t) = \sqrt{2}\, N_s^3 \, \langle \sigma_1(0)\, \sigma_1(t) \rangle$$

$$= \frac{N^2-1}{6\sqrt{2}\, N_s^3 N_t^2 \beta^2} \sum_{\substack{\vec{l} l_4 k_4 \\ (\vec{l}, l_4) \neq 0 \\ (\vec{l}, k_4) \neq 0}} \frac{\cos(l_4 t)\cos(k_4 t)}{\pi(\vec{l}, l_4)\pi(\vec{l}, k_4)} \cdot F(\gamma_1, \gamma_2, \gamma_3)$$

$$\sigma_1(t) = \frac{1}{\sqrt{2}\, N_s^3} \sum_{\vec{x}} \mathrm{Re}\, \frac{1}{N} \mathrm{Tr} \left(U(\dot{p}_{\vec{x},t}) - U(\dot{\tilde{p}}_{\vec{x},t}) \right)$$

$$F(\gamma_1, \gamma_2, \gamma_3) = 3(\gamma_1^2 + \gamma_2^2 + \gamma_3^2) + (\gamma_1 + \gamma_2 + \gamma_3)^2$$

$$\gamma_\lambda = 1 - \cos l_\lambda \quad .$$

The plaquette $\tilde{p}$ is obtained from p through a $\frac{\pi}{2}$ rotation.

Figure captions

Fig. 1: Prototyps of spacelike Wilson loops up to length 6.

Fig. 2: Different symmetry axis of the cube.

Fig. 3: All spacelike Wilson loops (up to opposite orientation) up to length 6.

Fig. 4: Prototyps of spacelike Wilson loops of length 8.

Fig. 5: Expectation values and their derivative.

5a: Operator #1 (Fig. 1): -, and operator #2 (Fig. 1): ---.

5b: Operator #3 (Fig. 1): -, operator #4 (Fig. 1): ---, and operator #1 (Fig. 4): ·····.

Fig. 6: Mass gap $m(0^{++})$ estimate.

6a: MC results for $\hat{m}_1(t)$, (t = 1,2) together with SC and spin wave results.

6b: MC results after minimization: $\hat{m}(t)$, (t = 1,2).

Fig. 7: MC results for the E^{++} representation: $m_1(1)$ and after minimization: $m(1)$. SC and spin wave results are also shown.

Operator # 1

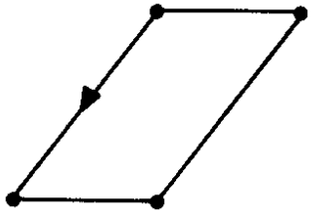

Operator # 2

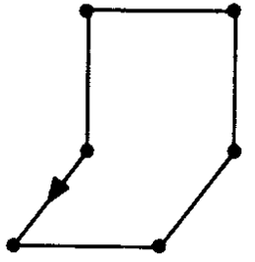

Operator # 3

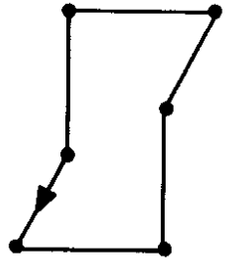

Operator # 4

Fig. 1

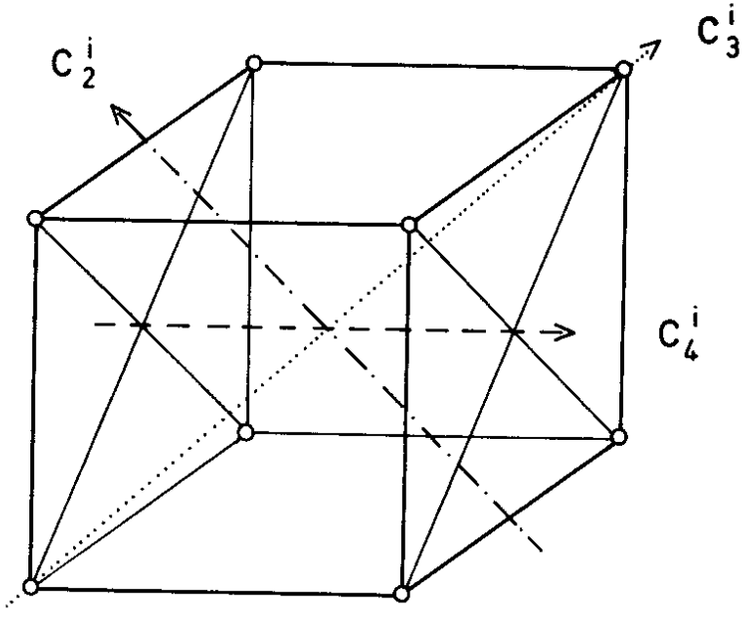

Fig. 2.

OPERATORS UP TO LENGTH 6

- used coordinate frame -

NOTATION :

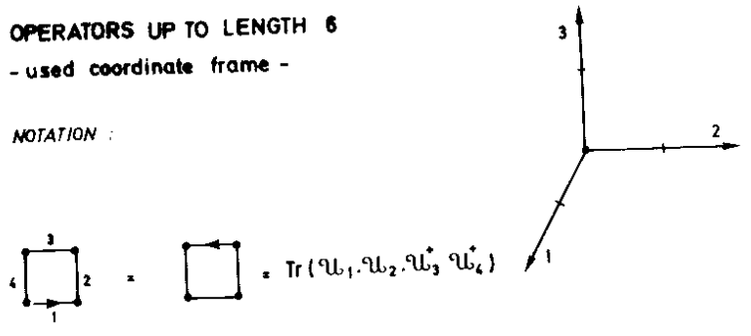

The 1-plaquettes -

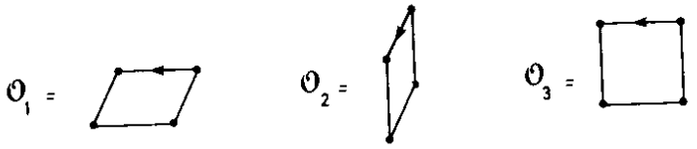

The double plaquettes -

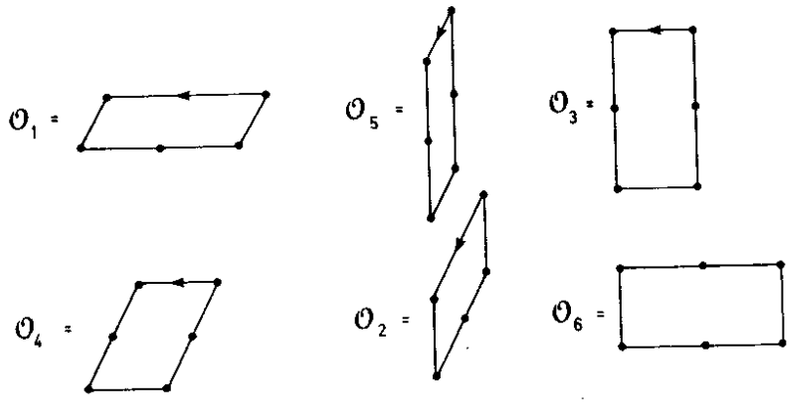

Fig.3

The bent plaquettes -

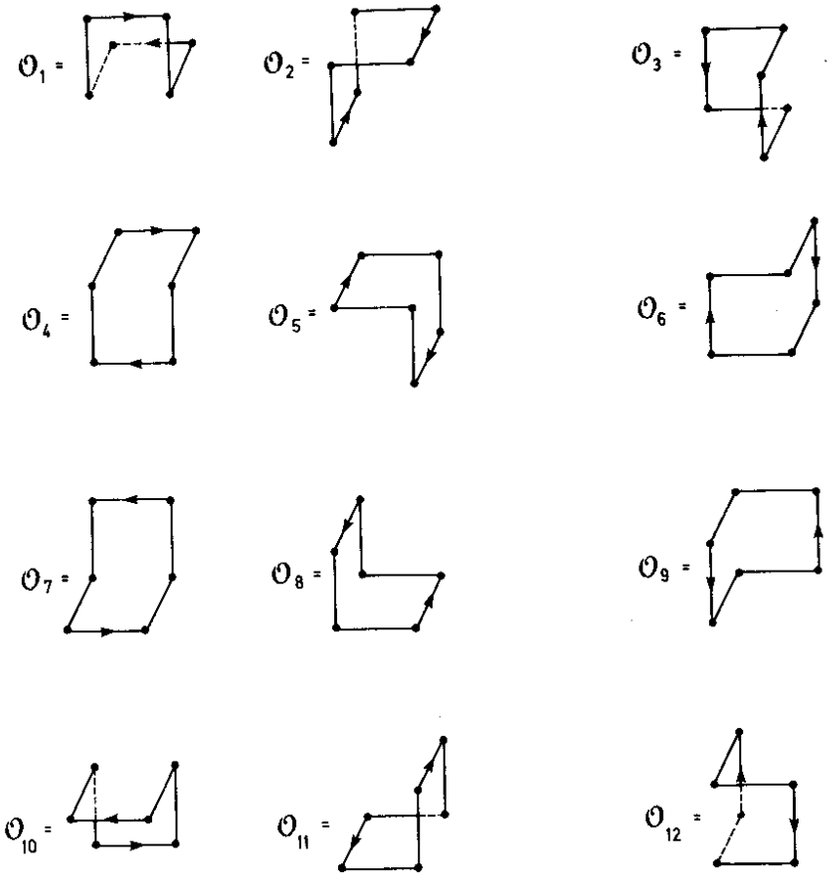

The twisted plaquettes -

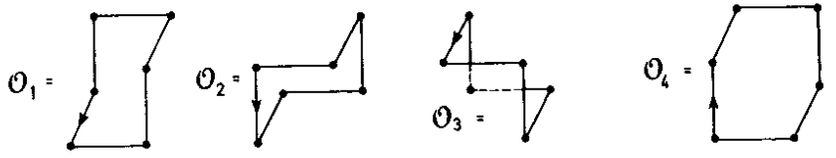

Fig.3

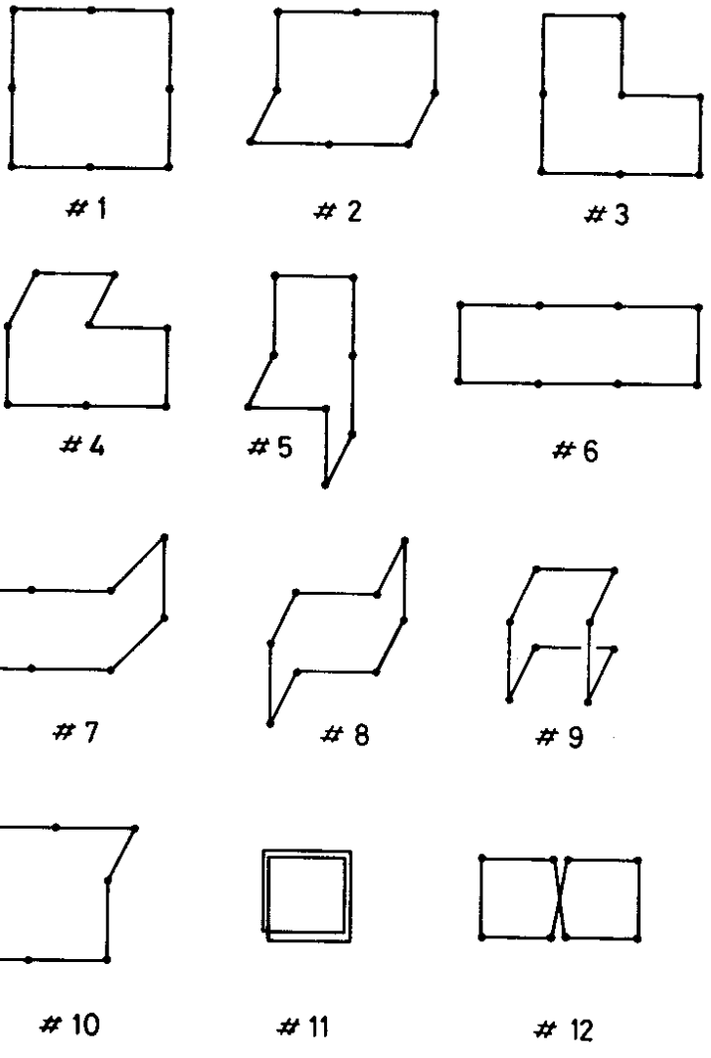

Fig. 4

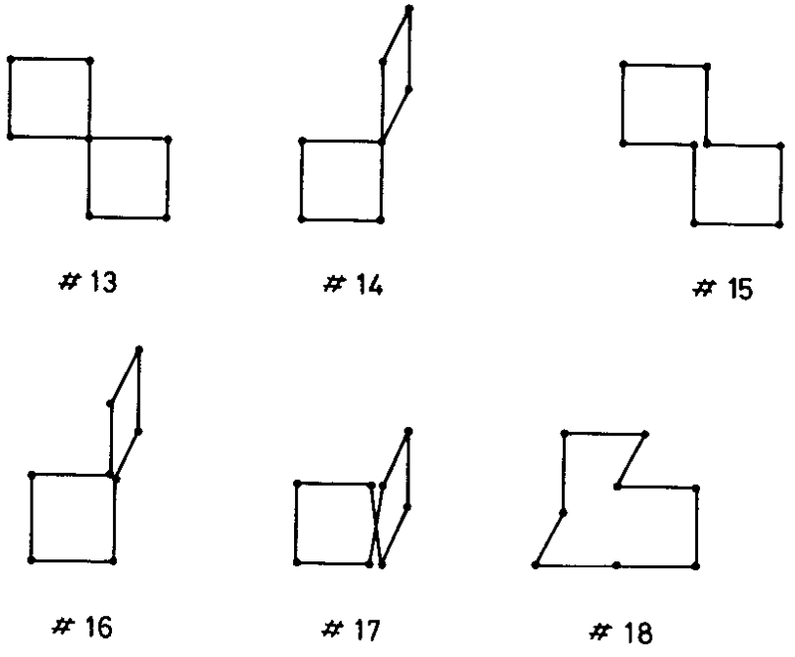

Fig. 4

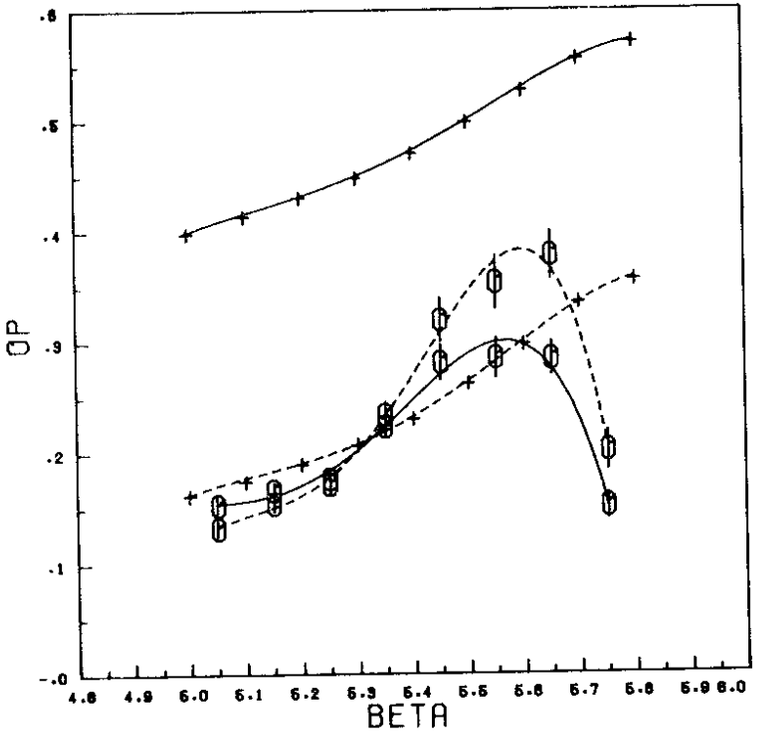

Fig. 5a

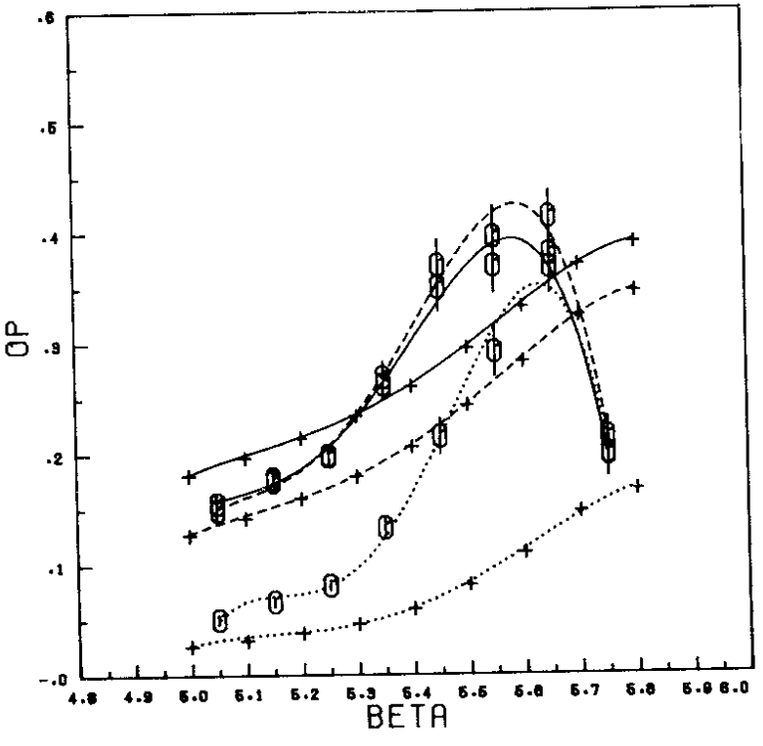

Fig. 5b

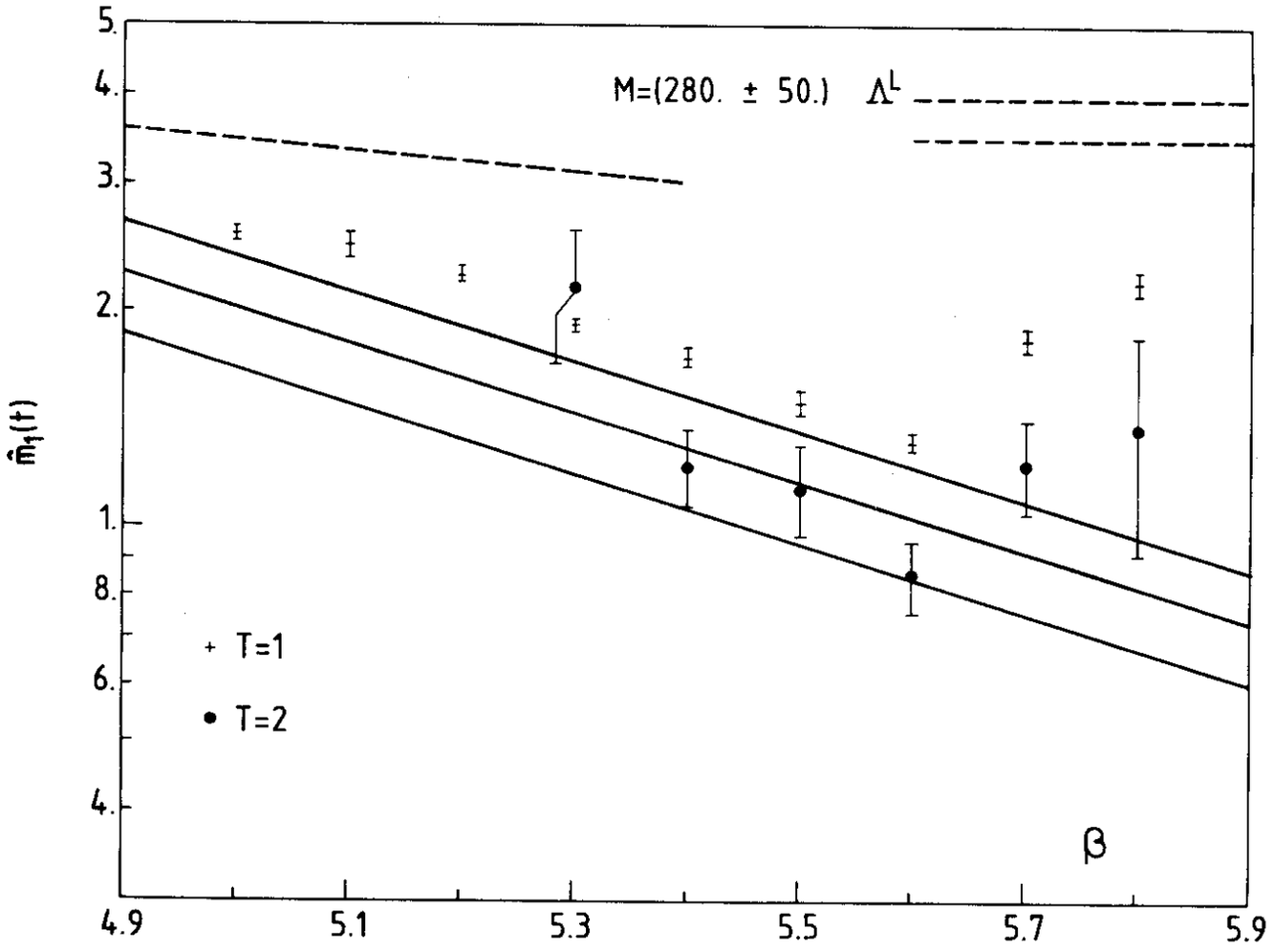
M=(280. ± 50.) Λ^L
$\hat{m}_1(t)$
+ T=1
• T=2
β
5.
4.
3.
2.
1.
8.
6.
4.
4.9
5.1
5.3
5.5
5.7
5.9

Fig. 6a

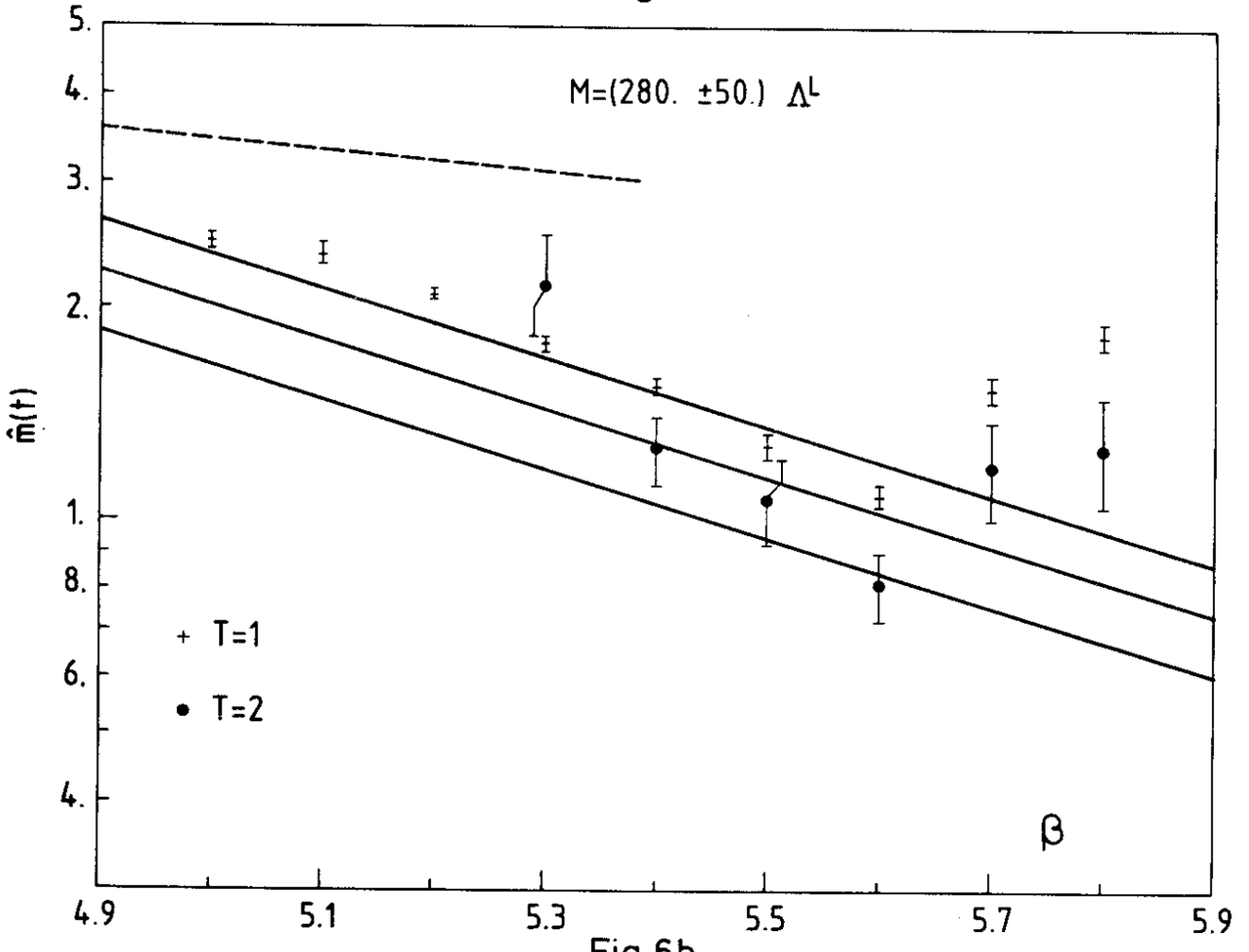
M=(280. ±50.) Λ^L
$\hat{m}(t)$
+ T=1
• T=2
β
5.
4.
3.
2.
1.
8.
6.
4.
4.9
5.1
5.3
5.5
5.7
5.9

Fig. 6b

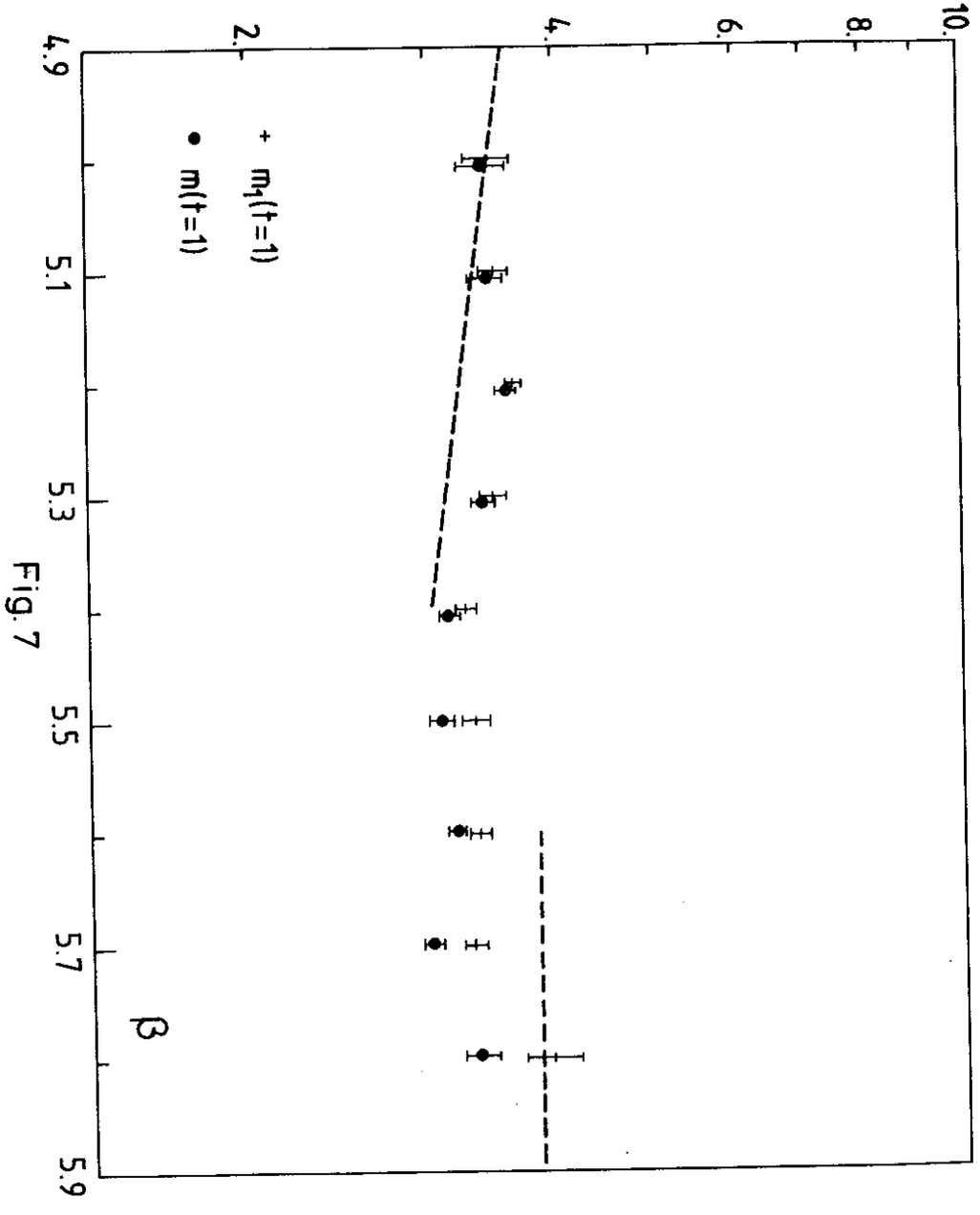

Fig. 7

	E	6 C_2	8 C_3	6 C_4	3 C_4^2
A_1	1	1	1	1	1
A_2	1	-1	1	-1	1
E	2	0	-1	0	2
T_1	3	-1	0	1	-1
T_2	3	1	0	-1	-1

Table 1

Character table for representations of the cubic group. The number in front of the symbol for the conjugate class gives the number of elements in this class.

R \ j	0	1	2	3	4	5	6	7	8	9	10	11	12
A_1	1	0	0	0	1	0	1	0	1	1	1	0	2
A_2	0	0	0	1	0	0	1	1	0	1	1	1	1
E	0	0	1	0	1	1	1	1	2	1	2	2	2
T_1	0	1	0	1	1	2	1	2	2	3	2	3	3
T_2	0	0	1	1	1	1	2	2	2	2	3	3	3

Table 2

Subduced representations of the rotation group up to J = 12 [28]. Given are the multiplicities with which the representation R can be found in the subduced representation D^{O}_{J}.

OP	d	A_1^{++}	A_2^{++}	E^{++}	T_1^{++}	T_2^{++}	A_1^{+-}	A_2^{+-}	E^{+-}	T_1^{+-}	T_2^{+-}
#1	6	1	0	1	0	0	0	0	0	1	0
#2	12	1	1	2	0	0	1	0	0	0	1
#3	24	1	0	1	0	1	0	0	0	1	1
#4	8	1	0	0	0	1	0	1	0	1	0
		A_1^{-+}	A_2^{-+}	E^{-+}	T_1^{-+}	T_2^{-+}	A_1^{--}	A_2^{--}	E^{--}	T_1^{--}	T_2^{--}
#3	24	0	0	0	1	1	1	0	1	0	1

Table 3.1

Irreducible contents of the representations of the symmetry group of the cube on Wilson loops up to length 6.

Table 4.1

Operator # 1

A_1^{++}	1		-2	1	
E^{++}	1	1	1		1
	1	-1	1		1
T_1^{+-}				1	

Wave function of the irreducible operators which can be built from 1-plaquette operators (e.g. $A_1^{++} = O_1 + O_2 + O_3$, first $E^{++} = O_2 - O_3$). According to $C = \pm 1$, the real or the imaginary part has to be taken. Suitable normalisation factors are understood.

Table 3.2 Reduction of representation on U classes of length 8 Wilson loops

OP	d	A_1^{++}	A_2^{++}	E^{++}	T_1^{++}	T_2^{++}	A_1^{-+}	A_2^{-+}	E^{-+}	T_1^{-+}	T_2^{-+}	A_1^{+-}	A_2^{+-}	E^{+-}	T_1^{+-}	T_2^{+-}	A_1^{--}	A_2^{--}	E^{--}	T_1^{--}	T_2^{--}
# 1	6	1	0	1	0	0	0	0	0	0	0	0	0	0	1	0	0	0	0	0	0
# 2	24	1	0	1	0	1	0	0	0	1	1	0	0	0	1	1	1	0	1	0	1
# 3	24	1	0	1	0	1	0	0	0	1	1	0	1	1	1	0	0	0	0	1	1
# 4	96	1	1	2	3	3	1	1	2	3	3	1	1	2	3	3	1	1	2	3	3
# 5	48	1	0	1	1	2	1	0	1	1	2	0	1	1	2	1	0	1	1	2	1
# 6	12	1	1	2	0	0	0	0	0	0	0	0	0	0	1	1	0	0	0	0	0
# 7	48	1	1	2	1	1	0	0	0	2	2	0	0	0	2	2	1	1	2	1	1
# 8	24	1	1	2	1	1	0	0	0	0	0	0	0	0	2	2	0	0	0	0	0
# 9	12	1	0	1	0	0	0	0	0	0	1	0	0	0	1	0	0	1	1	0	0
#10	24	1	0	1	1	2	0	0	0	0	0	0	1	1	2	1	0	0	0	0	0
#11	6	1	0	1	0	0	0	0	0	0	0	0	0	0	1	0	0	0	0	0	0
#12	12	1	1	2	0	0	0	0	0	0	0	0	0	0	0	0	0	0	0	1	1
#13	12	1	0	1	0	1	0	0	0	0	0	0	0	0	0	0	0	0	0	1	1
#14	48	1	0	1	1	2	1	0	1	1	2	0	1	1	2	1	0	1	1	2	1
#15	12	1	0	1	0	1	0	0	0	0	0	0	1	1	1	0	0	0	0	0	0
#16	48	1	0	1	1	2	1	0	1	1	2	1	0	1	1	2	1	0	1	1	2
#17	24	1	0	1	0	1	0	0	0	1	1	0	0	0	1	1	0	1	1	1	0
#18	96	1	1	2	3	3	1	1	**2**	3	3	1	1	2	3	3	1	1	2	3	3

Irreducible contents of the representations of the symmetry group of the cube on Wilson loops of length 8.

Table 4.2

Operator # 2

A_1^{++}	1	1	1	1	1	1
A_2^{++}	1	1	1	-1	-1	-1
E^{++}		1	-1		1	-1
	-2	1	1	-2	1	1
E^{++}	-2	1	1	2	-1	-1
		-1	1		1	-1
T_1^{+-}	1			1		
		1			1	
			1			1
T_2^{+-}	1			-1		
		1			-1	
			1			-1

Wave function of the irreducible operators one can build from the double plaquette operators.

Table 4.3

Operator # 3

A_1^{++} and A_1^{--}	1	1	1	1	1	1	1	1	1	1	1	1
E^{++} and E^{--}	-1	1		-1	1		-1	1		-1	1	
	-1	-1	2	-1	-1	2	-1	-1	2	-1	-1	2
T_1^{-+} and T_1^{+-}	-1	1		1	1		-1	-1		1	-1	
		-1	1		1	1		-1	-1		1	-1
	1		-1	1		1	-1		-1	-1		1
T_2^{-+} and T_2^{+-}	1	1		-1	1		1	-1		-1	-1	
		1	1		-1	1		1	-1		-1	-1
	1		1	1		-1	-1		1	-1		-1
T_2^{++} and T_2^{--}			1			-1			-1			1
	1			-1			-1			1		
		1			-1			-1			1	

Wave function of the irreducible operators one can build from bent plaquettes. (Note that through P: $0_1 \leftrightarrow 0_{10}^+$, $0_2 \leftrightarrow 0_{11}^+$, $0_3 \leftrightarrow 0_{12}^+$, $0_4 \leftrightarrow 0_7^+$, $0_5 \leftrightarrow 0_8^+$ and $0_6 \leftrightarrow 0_9^+$)

Table 5

β	# Sweeps	$\langle \sigma_1 \rangle$	$\langle \sigma_2 \rangle$	$\langle \sigma_3 \rangle$	$\langle \sigma_4 \rangle$
5.0	2800	.4000 ± .0003	.1628 ± .0002	.1824 ± .0003	.1284 ± .0004
5.1	2800	.4154 ± .0004	.1760 ± .0004	.1980 ± .0005	.1434 ± .0006
5.2	11200	.4320 ± .0003	.1914 ± .0003	.2158 ± .0003	.1609 ± .0004
5.3	5600	.4497 ± .0003	.2086 ± .0004	.2356 ± .0004	.1808 ± .0005
5.4	5600	.4715 ± .0005	.2314 ± .0005	.2612 ± .0006	.2070 ± .0006
5.5	5600	.4994 ± .0007	.2630 ± .0008	.2958 ± .0009	.2435 ± .0010
5.6	14000	.5290 ± .0008	.2997 ± .0011	.3341 ± .0011	.2846 ± .0013
5.7	5600	.5573 ± .0004	.3375 ± .0007	.3718 ± .0006	.3257 ± .0007
5.8	2800	.5720 ± .0006	.3568 ± .0011	.3910 ± .0009	.3464 ± .0011

Number of sweeps (R-upgrading) performed for each β value and vacuum expectation values for Wilson loops up to length 6. The normalization is $\langle \sigma_i \rangle \to 1$ for $\beta \to \infty$ (i = 1, ..., 4). Error bars are calculated by dividing all sweeps into 14 bins.

Table 4.4

Operator # 4

A_1^{++}, A_2^{+-}	1	-1	-1	-1
	1	1	1	-1
	1	-1	1	1
	1	1	-1	1
T_2^{++}, T_1^{+-}				

Wave functions of irreducible operators one can build from twisted plaquettes.

Table 7

β	c_1	c_2	c_3	c_4
5.2	.14 ± .04	− .44 ± .12	− .87 ± .28	− .16 ± .08
5.3	.09 ± .08	− .54 ± .19	− .82 ± .23	− .18 ± .13
5.4	.38 ± .04	− .56 ± .10	− .72 ± .06	− .15 ± .09
5.5	.56 ± .02	− .50 ± .04	− .65 ± .05	− .12 ± .04
5.6	.62 ± .01	− .49 ± .02	− .61 ± .02	− .04 ± .02
5.7	.66 ± .04	− .48 ± .04	− .58 ± .07	− .02 ± .06
5.8	.70 ± .08	− .59 ± .17	− .38 ± .09	− .14 ± .10

Best wave functions at distance t = 1.

Table 6

β	$m_1(1)$	$m_2(1)$	$m_3(1)$	$m_4(1)$	$m_g(1)$	$m_g(2)$	$\hat{m}_g(2)$
5.0	2.56 ± 0.06	2.70 ± 0.08	2.54 ± 0.08	2.70 ± 0.09	2.48 ± .06		
5.1	2.47 ± 0.09	2.56 ± 0.13	2.40 ± 0.09	2.55 ± 0.10	2.38 ± .08		
5.2	2.24 ± 0.05	2.29 ± 0.04	2.12 ± 0.04	2.23 ± 0.03	2.09 ± .04	2.39 ± .28	2.69 ± .55
5.3	1.93 ± 0.04	1.93 ± 0.04	1.82 ± 0.04	1.93 ± 0.05	1.79 ± .04	1.97 ± .19	2.15 ± .39
5.4	1.72 ± 0.04	1.67 ± 0.04	1.60 ± 0.04	1.67 ± 0.04	1.55 ± .04	1.40 ± .08	1.26 ± .14
5.5	1.49 ± 0.06	1.38 ± 0.05	1.34 ± 0.05	1.38 ± 0.05	1.28 ± .05	1.18 ± .09	1.08 ± .15
5.6	1.32 ± 0.04	1.17 ± 0.04	1.18 ± 0.04	1.21 ± 0.04	1.09 ± .04	.95 ± .05	.81 ± .09
5.7	1.83 ± 0.07	1.63 ± 0.07	1.67 ± 0.07	1.70 ± 0.06	1.54 ± .07	1.37 ± .11	1.19 ± .19
5.8	2.21 ± 0.08	1.94 ± 0.08	2.03 ± 0.08	2.05 ± 0.09	1.84 ± .08	1.55 ± .10	1.27 ± .22

Table 8

	OP	β = 5.2	β = 5.4	β = 5.6	β = 5.7
0^{--}	,3	> 5.70	> 6.41	4.54 ± .29	> 6.73
1^{+-}	1	6.10 ± 1.16	4.91 ± .46	5.40 ± .38	6.02 ± 1.07
	2	5.37 ± .52	4.26 ± .20	4.65 ± .10	4.98 ± .37
	3	5.23 ± .39	4.98 ± .54	4.72 ± .19	5.19 ± .50
	4	5.00 ± .29	5.51 ± .70	4.83 ± .19	5.32 ± .52
	Minimized	4.87 ± .44	4.19 ± .24	4.33 ± .16	4.56 ± .41
1^{-+}	,3	6.17 ± .89	6.51 ±1.87	5.78 ± .46	6.20 ± 1.51
2^{++}(E)	1	3.65 ± .07	3.27 ± .07	3.35 ± .08	3.30 ± .08
	2	3.67 ± .10	3.19 ± .08	3.20 ± .04	3.04 ± .07
	2	4.90 ± .30	4.40 ± .39	4.66 ± .20	4.12 ± .19
	3	4.11 ± .16	3.63 ± .12	3.55 ± .07	3.68 ± .15
	Minimized	3.58 ± .09	3.10 ± .07	3.11 ± .04	2.98 ± .07
2^{++}(T2)	3	4.77 ± .29	4.24 ± .16	3.74 ± .07	3.72 ± .14
	4	4.86 ± .25	4.34 ± .18	3.79 ± .07	3.78 ± .12
	Minimized	4.69 ± .24	4.14 ± .15	3.68 ± .06	3.66 ± .13
2^{+-}(T2)	3	5.65 ± .59	> 7.28	5.95 ± .65	5.56 ± .73
	4	⁄	5.23 ± .64	> 6.40	> 6.08
	Minimized	5.55 ± .48	5.12 ± .50	5.61 ± .44	5.33 ± .57
2^{-+}(T2)	,3	5.01 ± .29	4.65 ± .22	4.18 ± .11	4.10 ± .15
2^{--}(E)	,3	5.65 ± .59	> 6.62	6.41 ± .76	5.50 ± .45
2^{--}(T2)	,3	5.35 ± .28	6.68 ±1.78	5.95 ± .61	> 6.23
3^{++}	,2	5.79 ± .98	4.37 ± .41	4.54 ± .32	5.26 ± 1.08
3^{+-}	,4	> 5.59	4.81 ± .65	4.74 ± .30	> 5.31

Excited glueball states for several values of β (OP = contributing operator(s)).

Table 9

β	S-upgrading	R-upgrading
5.4	- 0.0043 ± 0.0060	- .0013 ± .0030
5.5	- 0.011 ± 0.0059	.0022 ± .0062
5.7	- 0.0080 ± 0.0070	- .0035 ± .0048

Comparison of S- and R-upgrading results for 0^{--} correlations. In case of S-upgrading each result relies on 2000 sweeps and error bars are calculated with respect to 10 bins of 200 sweeps. (In case of R-upgrading as in Table 5.)

Table 11

Glueball masses from finite distance correlation function in the spin wave approximation on an $4^3 \cdot 8$ lattice.

	0^{++}		$2^{++}(E)$	
	m(t)	$\hat{m}(t)$	m(t)	$\hat{m}(t)$
t = 1	3.96	3.96	3.83	3.83
t = 2	3.72	3.48	3.58	3.33
t = 3	3.47	2.95	3.33	2.83

Table 10

	5.0	5.1	5.2	5.3	5.4	5.5	5.6	5.7	5.8
$m_1^{T_1^{+-}}(1)/m_1^{A_1^{++}}(1)$	2.10 ± 0.26	1.97 ± 0.16	2.71 ± 0.44	3.09 ± 0.49	2.94 ± 0.32	3.21 ± 0.14	4.23 ± 0.16	3.43 ± 0.65	2.56 ± 0.87
$m_1^{E^{++}}(1)/m_1^{A_1^{++}}(1)$	1.35 ± 0.07	1.42 ± 0.05	1.63 ± 0.03	1.79 ± 0.07	1.90 ± 0.05	2.23 ± 0.08	2.55 ± 0.07	1.80 ± 0.05	1.78 ± 0.1

The fractions $m_1^{T_1^{+-}}(1)/m_1^{A_1^{++}}(1)$ and $m_1^{E^{++}}(1)/m_1^{A_1^{++}}(1)$ are given as function of β. We have devided by the mean values for $m_1^{A_1^{++}}(1)$ (Table 6) and taken the error bars of $m_1^{T_1^{+-}}(1)$, $m_1^{E^{++}}(1)$ respectively.